HYDROGEOCHEMICAL MODELING

OF WESTERN MOUNTAIN FRONT RECHARGE,

UPPER CIENEGA CREEK SUB-BASIN,

PIMA COUNTY, ARIZONA

by

Hans Jarlath Huth

A Thesis Submitted to the Faculty of the

DEPARTMENT OF HYDROLOGY AND WATER RESOURCES

In Partial Fulfillment of the Requirements
For the Degree of

MASTER OF SCIENCE
WITH A MAJOR IN HYDROLOGY

In the Graduate College

THE UNIVERSITY OF ARIZONA

1996

TABLE OF CONTENTS

front recharge is considered to be the major component of aquifer recharge. Harshbarger and Associates (1985) calculated 6,000 acre-feet/yr of mountain front recharge for the upper basin using estimates from previous studies.

Two wells located along the Empire Gulch drainage (Well ID 68 and 70, Appendix 1) located downgradient of Empire Gulch Springs are flowing wells. However, these both have artesian heads of approximately the same level as static water levels in nearby unconfined wells (highlighted in Appendix 2). There is no basis for assuming that confined or semi-confined conditions are present within the valley since other wells do not repeat these artesian conditions. For this reason, the upper basin aquifer is considered to be regionally unconfined, and all wells within the basin are assumed to represent the same regional aquifer.
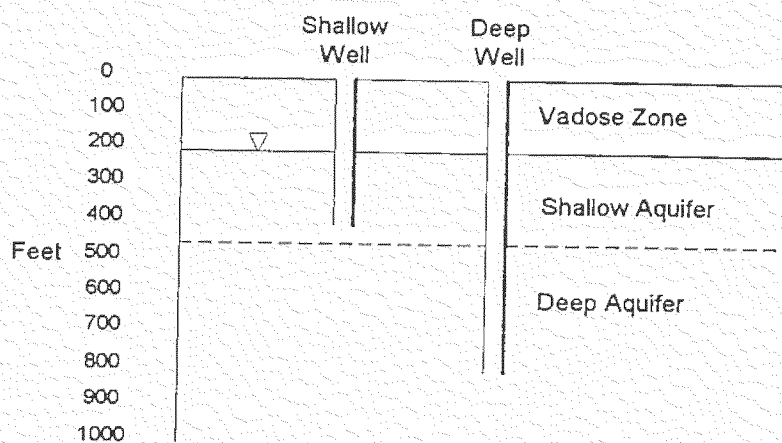
Figure 3.4 Examples for Well Classification

The criterion for these definitions is arbitrary. According to driller's logs

(Harshbargar and Associates, 1975), there are no strata to indicate that a physical

separation exists between the shallow and deep aquifer as defined in this study. Robertson

(1991) observed that, in most basins of the southwest, concentrations of magnesium,

bicarbonate, and silica decrease with depth down to 2,000 feet while pH, temperature, and

the majority of trace metals are observed to increase with depth. Calcium generally, but

not invariably, also decreases with depth (Robertson, 1991).

Three field samples were collected and analyzed to identify the extent of water

quality changes with respect to drilling depth. These analyses represent waters of different

depths all located within a one-mile radius of one another in the Empire Ranch area

(T19S, R16E, sec 18). These sites were chosen in order to minimize chemical differences

resulting from areal distributions. Site 19 (Empire Gulch Springs) represents a headward
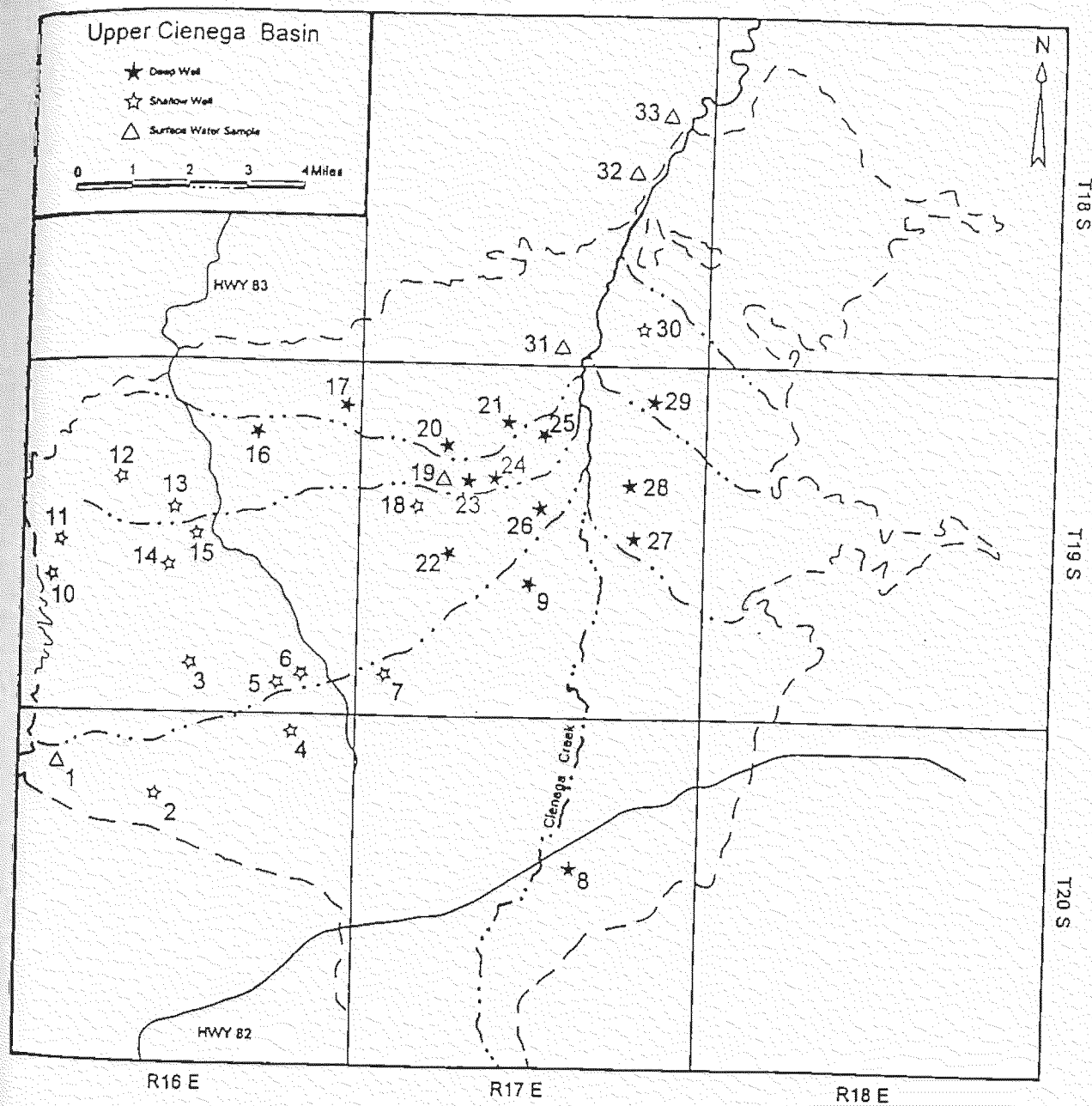
Figure 3.5 Geographic Distribution of Deep and Shallow Wells

recharge and older waters within the regional aquifer.

An alternative explanation is that differences in chemistry result from the areal distribution of analyses as opposed to depth. This is supported by the non-uniform distribution of deep and shallow wells within the basin. As demonstrated by Figure 3.5, deep wells are located within a four-mile corridor surrounding Cienega Creek whereas shallow wells are characteristic of mountain front recharge. The high sodium concentration for the deep wells may result from cation exchange mechanisms being more significant within the central basin as compared to the mountain front. This is supported by relatively lower magnesium concentrations within the central basin along with increases in sodium, both of which suggest magnesium-sodium cation exchange. In addition, central basin waters may represent dilute recharge from the Pleistocene Epoch whereas mountain front recharge may represent recent recharge affected by evaporation. This supports areal differences in chloride.

Given the available information, it is unclear whether differences in water analyses are more significantly affected by depth or areal distribution. Either hypothesis should be checked by installing a nest of piezometers in the area of question in an attempt to check for (the lack of) a vertical gradient in the Empire Ranch area. For the purposes of this study, because the distribution of wells does not allow for the exclusive modeling of a deep or shallow flowroute, flowpaths will be classified as evolving waters along (a) the shallow aquifer, (b) the deep aquifer, or (c) shallow to deep aquifer. It is assumed that

SI are then derived from these activities in order to determine the saturation state for minerals at endmember wells. If SI indicates that a mineral is significantly undersaturated or supersaturated for two wells defining a flowpath, then all models indicating respective precipitation or dissolution for this mineral may be eliminated. Where starting and ending wells demonstrate both supersaturation and undersaturation for a mineral, no model may be excluded based on the activity of this mineral. The use of SI constraints eliminates some, but not all, models from the solution set. As such, the final solution set is still non-unique. Because isotopic data are not available, chemical intuition and assumptions about the geology of the flowpath are used to identify the most representative flowpath.

Modeling Assumptions

1. Wells defining a flowpath contain waters which are related to one another by the hydrologic gradient associated with the flowpath.

2. The aquifer contains significant amounts of oxygen irrespective of location or depth as was found by Robertson (1991).

3. Any reduced iron in solution is readily oxidized to goethite. Therefore, iron is conserved and not considered an analytical constraint.

4. Both aluminum and potassium are readily incorporated into the weathering products of clays (Hem, 1992). Therefore, these are conserved and not considered to be analytical constraints.

5. All increases in sulfur are derived from dissolution of gypsum ($CaSO_4$) or anhydrite ($CaSO_4$)·$2H_2O$, both of which are considered identical for purposes of mass balance modeling.

6. Carbonate minerals and cation exchange are the only sources and sinks for calcium and magnesium. Contributions from the dissolution of felsic minerals are relatively insignificant.

7. Carbonate minerals and $CO_2(g)$ fluxes account for all sources and sinks of carbon; contributions from organic carbon are insignificant.

8. Chloride is assumed to act conservatively. Any changes in chloride result from infiltration or mixing with dilute waters. Infiltrating or mixing waters assumed to be dilute in all other constituents.

9. Infiltration is confined to the mountain front. Any precipitation taking place within the valley alluvium is lost to evapotranspiration.

10. Calcium-sodium and magnesium-sodium cation exchange are the only sources for increases in sodium concentrations; contributions to sodium from the dissolution of felsic minerals or halite are relatively insignificant.

11. Thermodynamic constants are valid for the temperature range characteristic of Basin groundwaters.

12. Minerals for which mass transfer and saturation indices are calculated dissolve congruently. This does not include the weathering of silicates which are not modeled given lack of analyses of SiO_2.

CHAPTER 4
FLOWPATH MODELING OF WESTERN BASIN RECHARGE

Due to the relative geographic distribution of shallow and deep wells as defined in this study (Figure 3.5), the following flowroutes characterize the evolution of shallow mountain front recharge to deep waters of the central basin. No shallow wells are available for modeling within the central basin.

Modeled flowroutes follow the axes of important drainages including Gardner Canyon in the south, Empire Gulch in the mid-west, and Oak Tree Canyon in the north (Figure 4.1). Each flowroute is divided into a series of shorter flowpaths based on the availability of chemical analyses. Flowroutes are modeled until mass balance forces violations of thermodynamic constraints. When these violations cannot be resolved through mixing of flowpaths, mixing of more than two waters is assumed to take place and modeling is suspended.

In this study, analyses for endmember wells are presented as mmol/l (originally entered into NETPATH as meq/l from charge balance tables). When valid models are generated, NETPATH reports phase contributions as mmol/l transferred into or out of an evolving groundwater. Negative values indicate precipitation or loss of a phase from groundwater, whereas positive numbers indicate dissolution into groundwater. Only valid thermodynamic models are presented. When more than one model is generated, none can be excluded without making assumptions about the geology and/or the mineralogy of the area.

Flowroute 1
Gardner Canyon Recharge

Flowroute 1 originates at the mountain front of Gardner Canyon and follows the trough of the canyon for 10 miles (Figure 4.1). At the start of the flowpath, Gardner Canyon intersects the southwest-trending Sawmill Canyon Fault Zone (Drewes, 1972). This fault zone separates the central tectonic block of the Santa Rita Mountains from its northeastern arm and contains extensive deposits of limestone, dolomite, siltstone, and shales representing the Lower Permian Naco group (Drewes, 1972). The mountain front contains extensive dolostone outcrops and coarse alluvial deposits.

Traveling northeast for five miles from the mountain front, Gardner Canyon bisects Highway 83. Dark reddish soils are made visible in roadcuts along the highway. East of Highway 83, the gradient of Gardner Canyon flattens out, but alluvial deposits along the axis of Gardner Canyon remain relatively coarse. The potentiometric surface is less than 50 feet below the land surface along the entire gradient of this flowroute (ADWR, 1995).

Flowpath 1
Shallow Gardner Canyon Alluvium

Flowpath 1 originates at the southwestern foothills of the Santa Ritas north of the groundwater divide with the Sonoita Basin. This flowpath traverses 4.8 miles of sands and gravels tracing the low elevation contour of Gardner Canyon. The starting endmember is a spring located on the premises of Apache Springs Ranch (Site 1).
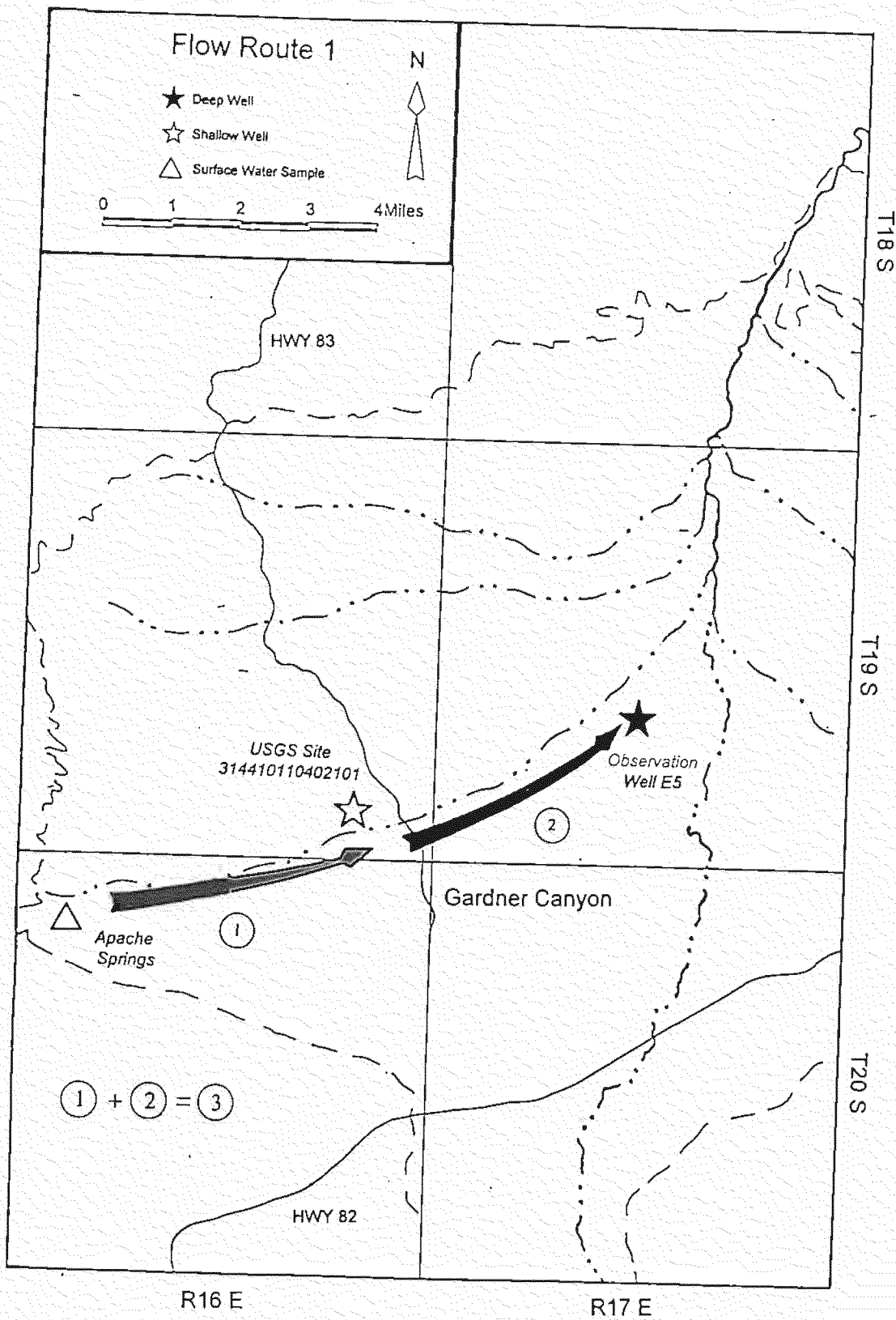
Figure 4.1 Flowroute 1: Gardner Canyon Recharge

This spring is located inside a small shed and is cased for 10 feet (ADWR, 1995). The water level is 2 feet beneath the land surface (ADWR, 1995). The mineralogy surrounding this spring is characterized by large dolomitic outcrops containing thin veins of calcite.

As a final endmember, sites 4, 5, and 6 are located at the end of the flowpath (Figure 3.5). These are less than one-half mile away from one another with the water level less than 50 feet beneath the land surface (USGS-WRC, 1995). Well depths for this vicinity average 140 feet (ADWR, 1995). The shallow water depth coupled with the coarse nature of the Canyon's alluvium suggest recharge of flood flows along the gradient.

The USGS data set contained no pH measurements for sites 4, 5, and 6. Field activities located one well in this area with no means for sampling. A search of the USGS-DDS 18-A database identified three pH measurements of 7.6 for locations 2.5 miles downgradient (T19S, R17E, sections 26 and 31). No major cation/anion analyses were included with these pH readings.

Assuming that weathering of silicates generate increases in pH along the gradient of Gardner Canyon, the missing pH values for the endmember wells are hypothesized to range between 7.2 and 7.6. If it is assumed that groundwaters are maintaining equilibrium with the calcite through precipitation, a pH of 7.6 generates an almost perfect equilibrium with calcite for endmember 4. This pH is used accordingly. Table 4.1 shows the chemical budget for Flowpath 1.

Table 4.1: Route1, Path 1: Upper Gardner Canyon Alluvium Chemical Budget (mmol/l)

Endmembers	Ca^{+2}	Mg^{+2}	Na^+	SO_4^{2-}	HCO_3^-	Cl^-	SI Calcite	SI Dolomite	SI Gypsum	pH
Apache Springs (Site 1)	1.95	0.99	0.43	0.05	5.08	0.20	0.249	-0.326	-2.873	7.40
314410110401001 (Site 4)	1.05	0.34	0.43	0.08	2.48	0.11	-0.001	-1.006	-2.825	7.60
Change	-0.90	-0.65	0.00	0.03	-2.60	-0.09	-0.250	-0.680	-0.048	0.20

The loss of chloride (0.09 mmol/l) corroborates dilution of groundwaters through infiltration of summer flood flows. Since mixing ratios are based on the chloride concentrations, a concentration must be assumed for infiltrating waters. The Walnut Gulch Experimental Watershed near Tombstone, Arizona (about 30 miles east of Cienega Creek Basin), averages 0.5 mg/l, or 0.014 mmol/l for chloride (Simpson, 1983). An analysis of rainfall in Tucson, Arizona shows a concentration of 6 mg/l, or 0.169 mmol/l (Simpson, 1983). The high value of the Tucson measurement may be ascribed to local atmospheric pollution (Simpson, 1983). Snow collected from Mount Wrightson in the Santa Rita Mountains demonstrates a chloride concentration of 1 mg/l, or 0.028 mmol/l. There are many processes that could affect the representative nature of this measurement. Assuming snow is representative of precipitation, a chloride concentration of 1 mg/l (0.028 mmol/l) is used as an approximation for infiltrating waters. Under these assumptions, six models were generated incorporating infiltration along the gradient (Table 4.2).

Table 4.2: Route1, Path 1: Upper Gardner Canyon Models
(0.028 mmol/l Chloride Infiltration)

PHASE	1	2	3	4	5[1]	6
Apache Spr.	47%	47%	47%	47%	47%	47%
Infiltration	53%	53%	53%	53%	53%	53%
Calcite	0.07130	0.07130	0.07130			
Dolomite				0.03565	**0.03565**	0.03565
Gypsum	0.05149	0.05149	0.05149	0.05149	**0.05149**	0.05149
CO_2	-0.01978	-0.01978	-0.01978	-0.01978	**-0.01978**	-0.01978
X-Ca-Na	0.11386		-0.01201	0.11386		-0.04766
X-Ca-Mg	-0.12587	-0.01201		-0.16152	**-0.04766**	
X-Mg-Na		0.11386	0.12587		**0.11386**	0.16152

[1]Bold indicates selected model(s).

The results from these models demonstrate a significant 53% dilution factor for flow along the 5-mile gradient. As a check for the assumed chloride concentration of infiltrating waters (0.028 mmol/l), NETPATH was run a second time using a chloride concentration of 0.014 mmol/l characteristic of the Walnut Gulch Experimental Watershed. Respective mass balance models were almost identical demonstrating only a 4% decrease in the contribution of infiltration along the gradient. The coarse nature of the alluvium near the mountain front and associated summer flood flows support the large dilution factor. If this is the case, it must be assumed that chemical contributions from mixing flowpaths are dilute in all other chemical constituents; a reasonable assumption given the close proximity of these wells to the mountain front.

For the six models presented in Table 5, Models 1 through 3 demonstrate exclusive calcite dissolution (0.071 mmol/l), while 4 through 6 incorporate dolomite dissolution (0.036 mmol/l). Calcite dissolution is questionable given the significant

amount of supersaturation for this mineral at Apache Springs (Site 1) and the assumed pH

(7.6) for Well 314410110401001 (Site 4). Undersaturation of dolomite suggests

dissolution of this mineral. For the three models demonstrating dolomite dissolution,

Model 5 requires the least amount of cation exchange. The relatively close location of this

canyon to the mountain front is unfavorable for clay deposition. For these reasons, Model

5 is chosen to represent this flowpath; however, the other models may be valid given the

paucity of the data.

Exclusive calcium-sodium or magnesium-sodium cation exchange in these and

other models results from the inclusion of a calcium-magnesium exchange phase.

Inclusion of this phase in the database is convenient for increasing the probability of

convergence on a solution as required by the analytical uncertainties of the data.

Nevertheless, it is more likely that calcium and magnesium are both exchanging for sodium

concurrently rather than exclusively. For this reason, proposed cation exchange

contributions are qualitative at best.

Flowpath 2
Lower Gardner Canyon Alluvium

Flowpath 2 is a continuation of the Gardner Canyon flowroute. It begins at Well

314410110401001 (Site 4) and evolves for 4.5 miles through coarse-grained alluvium

where it finally terminates at Well E5 (Site 9). Table 4.3 shows the chemical budget.

Table 4.3: Route1, Path 2: Lower Gardner Canyon Chemical Budget (mmol/l)

Endmembers	Ca⁺²	Mg⁺²	Na⁺	SO₄²⁻	HCO₃⁻	Cl⁻	SI Calcite	SI Dolomite	SI Gypsum	pH
314410110401001 (Site 4)	1.05	0.34	0.43	0.08	2.48	0.11	-0.001	-1.006	-2.825	7.60
Well E5 (Site 9)	0.68	0.26	1.74	0.14	3.24	0.11	-0.022	-0.358	-2.748	7.70
Change	-0.37	-0.08	1.31	0.06	0.76	0.00	-0.021	0.702	0.077	0.10

The depth to water for the final endmember Well E5 (Site 9) is only 54 feet below the surface (Harshbarger and Associates, 1978). The well is cased solid, however, for 300 feet followed by an 800-foot screening interval (Harshbarger and Associates, 1978). For this reason, it is assumed that the final endmember represents waters from a deeper portion of the basin alluvium. Because there is no chemical information for shallow wells at the terminus of this flowpath, this well is the only option for modeling. Due to the deep screening interval of the endmember well, it is assumed that models describe the evolution of shallow waters to the deeper aquifer.

Conservation of chloride results in no mixing adjustments for this chemical budget. Seven models were generated and are presented in Table 4.4. Of the seven models, results from six demonstrate calcite dissolution. Only the results from one model shows calcite precipitating.

Table 4.4: Route1, Path 2: Lower Gardner Canyon Models (mmol/l)

PHASE	1[1]	2	3	4	5	6	7
Calcite	-1.00526	0.13514	0.13514	0.13514			
Dolomite	0.57020				0.06757	0.06757	0.06757
Gypsum	0.06002	0.06002	0.06002	0.06002	0.06002	0.06002	0.06002
CO_2	0.63787	0.63787	0.63787	0.63787	0.63787	0.63787	0.63787
X-Ca-Na		0.65520		0.57020	0.65520		0.50263
X-Ca-Mg		-0.08500	0.57020		-0.15257	0.50263	
X-Mg-Na	0.65520		0.65520	0.08500		0.65520	0.15257

[1]Bold indicates selected model(s).

These seven results suggest three mechanisms for decreases in calcium. Due to pH increases, Model 1 are for calcite precipitation (-1.005 mmol/l). Results from Models 2 through 4 are for cation exchange on clays in conjunction with dissolution of calcite. Models 5 and 6 exclude calcite as a phase, suggesting that cation exchange is contributing to the observed equilibrium for calcite at Well E5 (Site 9). No model may be discarded due to the lack of a measured pH at Well 314410110401001 (Site 4). All models demonstrate a greater contribution of cation exchange for increases in sodium as compared to Flowpath 1. This is reasonable given the shallow surface gradients in this area. Assuming calcite precipitation is resulting from increases in pH, Model 1 is chosen to represent this flowpath.

Flowpath 3
Gardner Canyon Deep Groundwater Evolution

Given the uncertainties relating to Flowpath 2, the following model is an
alternative for the modeling of deep waters evolution along Gardner Canyon. This
flowpath differs from Flowpath 2 in that the evolution to the central basin (Site 9) begins
from Apache Springs (Site 1) rather than Well 314410110401001(Site 4). This flowpath
assumes that deep basin waters in the western half of the basin originate from mountain
front recharge along the Santa Ritas. Because of chloride dilution, infiltration near the
mountain front is assumed. Table 4.5 present the chemical budget and flowpath.

Table 4.5: Route1, Path 3: Deep Groundwater Chemical Budget (mmol/l)

Endmembers	Ca^{+2}	Mg^{+2}	Na^+	SO_4^{2-}	HCO_3	Cl^-	SI Calcite	SI Dolomite	SI Gypsum	pH
Apache Springs (Site 1)	1.95	0.99	0.43	0.05	5.08	0.20	0.249	-0.326	-2.873	7.40
Well E5 (Site 9)	0.68	0.26	1.74	0.14	3.24	0.11	-0.022	-0.358	-2.748	7.70
Change	-1.27	-0.73	1.31	0.09	1.84	-0.09	-0.227	-0.032	-0.125	0.30

Table 4.6 presents the resulting mass balance models which account for infiltration with

waters containing the assumed 0.028 mmol/l chloride.

Table 4.6: Route1, Path 3: Deep Groundwater Models
(0.028 mmol/l Chloride Infiltration)

PHASE	1	2	3	4[1]
Site 1	72%	72%	72%	72%
Infiltration	23%	23%	23%	23%
Calcite	-1.27625	-0.36413	-0.36413	-0.36413
Dolomite	0.45606			
Gypsum	0.06593	0.06593	0.06593	0.06593
CO_2	-0.19849	-0.19849	-0.19849	-0.19849
X-Ca-Na		0.76477		0.45606
X-Ca-Mg		-0.30871	0.45606	
X-Mg-Na	0.76477		0.76477	0.30871

[1]Bold indicates selected model(s).

The results of these models are similar to those of Flowpath 2 in that they demonstrate a

large contribution of cation exchange to account for the observed increases in sodium.

The difference is with respect to infiltration which is more reasonable for this flowpath

(23%). The results of the models demonstrate net precipitation of calcite, which is

reasonable given the supersaturation observed at Site 1 and subsequent increases in pH.

The distinguishing feature between models is the inclusion of dolomite as a phase in

Model 1. Contributions to calcium concentration from dolomite dissolution

(0.456 mmol/l) require larger contributions of calcite precipitation to account for mass

balance on calcium. The only remaining difference between the models is the different

cation exchange mechanisms, all of which are reasonable. However, large calcium and

magnesium concentrations relative to sodium in suggest exchange of divalent cations for

monovalent sodium on clay surfaces. For this reason, Model 4 is chosen to represent this flowpath.

Gardner Canyon and Empire Gulch
Deep Aquifer Mixing

Endmembers downgradient of Well E5 (Site 9) cannot be created without considering mixing from other wells. The loss of sulfate between Well E5 (Site 9) to Well E8 (Site 26) cannot be modeled through precipitation of undersaturated gypsum. No other data for endmembers exclusive to the Gardner Canyon flowroute are available, but the evolution of Well E9 (Site 25) at the confluence of Gardner Canyon and Empire Gulch can be modeled if mixing from the Empire Gulch Well (Site 24) is included (Figure 4.2).

The Empire Gulch Well (Site 24) is located near the BLM-owned Empire Ranch. This well is drilled for 845 feet (ADWR, 1995) and is assumed to represent deep aquifer waters due to its respective shallow head (surface). The analysis for Well E9 (Site 25) is assumed to represent the deeper aquifer resulting from its depth of 1,400 feet (Harshbarger and Associates, 1978). The deep aquifer characteristics of Well E5 (Site 9) were discussed in the section for Flowpath 2. The mixing chemical budget and mixing models presented in Table 4.7 and 4.8 respectively are assumed to represent mixing of deep aquifer waters.
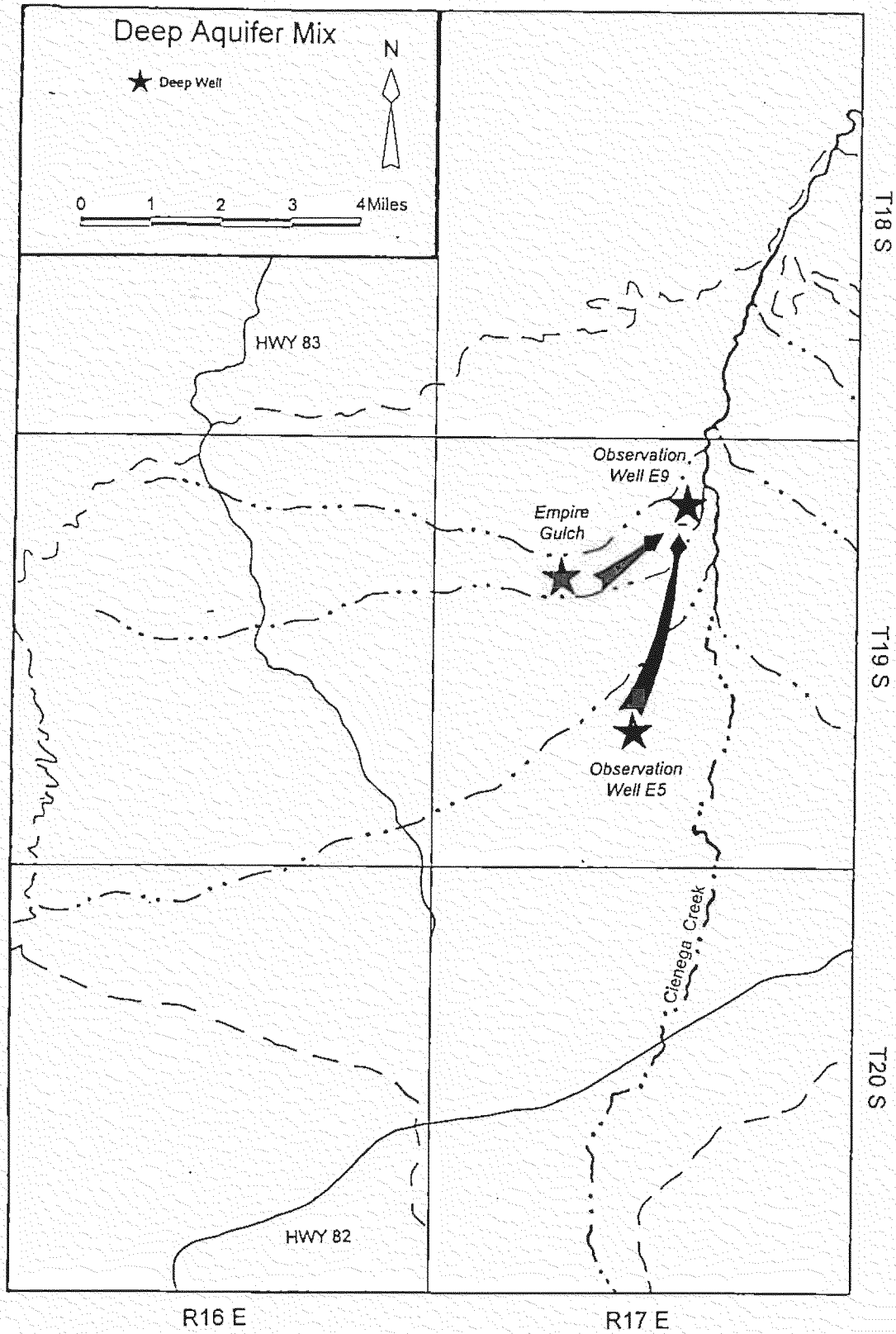
Figure 4.2 Deep Aquifer Mix: Gardner Canyon - Empire Gulch

Common to the results for all three models in Table 4.8 is the degassing of CO_2 (-0.630 mmol/l). This suggests that either a third water type dilute in CO_2 is mixing with the final endmember, or actual degassing may have occurred in the lab prior to sample analysis. The latter would explain the anomalous high pH for Well E9. If this is the case, then supersaturation calculated for Well E9 may be artificial (SI = 0.123). Decreasing the pH down to 8.26 in order to account for the CO_2 loss would establish equilibrium with this mineral (SI = -0.008). Likewise, corrections for CO_2 out-gassing would minimize the unlikely large losses of CO_2 reported in the model.

Mixing of waters undersaturated with calcium and losses of calcium on clays suggest that calcium dissolution is necessary to create the hypothesized equilibrium at the Well E9. Model 2 is the most reasonable for this hypothesis demonstrating calcite dissolution (0.142 mmol/l). Conversely, if the pH for Well E9 is correct, then supersaturation for calcite at Well E9 corroborates calcite precipitation (-1.083 mmol/l) as demonstrated by the results from Model 1. Without information regarding field sampling protocol, it will be assumed that the analyses are representative of actual groundwater conditions. For this reason, Model 1 is selected to represent this mixing scenario.

Flowroute 2
Empire Gulch Recharge

This flowpath represents the shallow aquifer dynamics taking place along a five-mile gradient of the Empire Gulch (Figure 4.3). Field visits to Greaterville area west of the Empire Gulch observed significant amounts of limestone, azurite, and dolomite exposed in primitive road cuts along the mountain front. Geologic maps of the mountain area west of Greaterville demonstrate rhyolite porphyry dikes (Drewes, 1972). These are hypothesized to provide the source of copper necessary for the observed azurite deposit. This mineral is also common to other locations in Arizona including Bisbee and Morenci (Klein and Hurlbut, 1993). At higher elevations, continental granodiorites and associated sandstones dominate the terrain. Field visits revealed small pyrite crystals in these sandstones stained red from oxidation.

Flowpath 4
Empire Gulch Shallow Aquifer Evolution

This flowpath traverses the five mile gradient of Empire Gulch before terminating at the central basin margin surrounding the Cienega Creek corridor (Figure 4.3). Well 314638110423401 (Site 13) and the Empire Ranch Well (Site 18) are drilled for 365 and 220 feet respectively (USGS-WRC, 1995; ADWR, 1996). These demonstrate a high chloride signature (0.37and 0.29 mmol/l) characteristic of other shallow wells along this gradient (See Appendix 5 for full summary of shallow wells). The chemical budget for this flowpath is presented in Table 4.9.
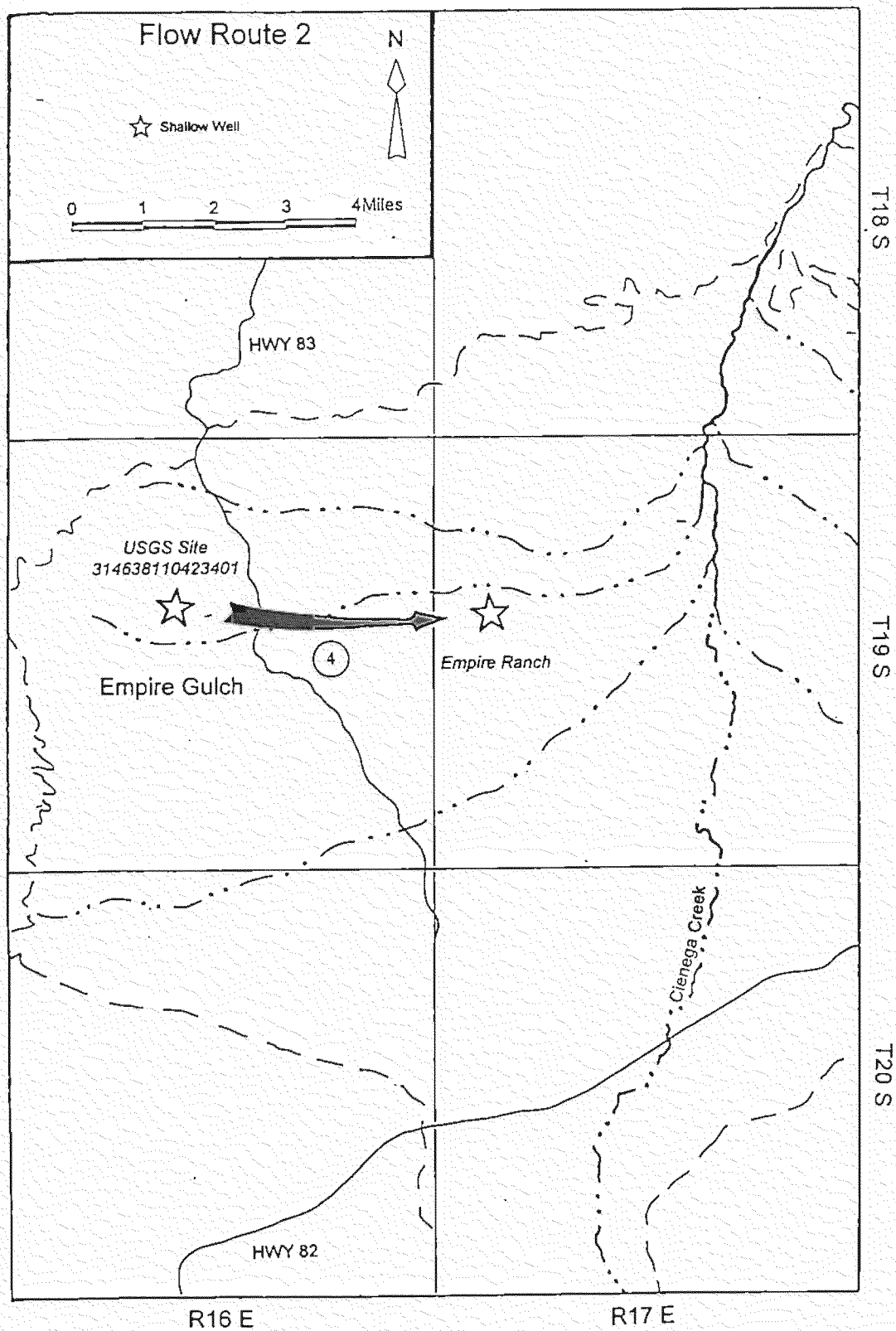
Figure 4.3 Flowroute 2: Empire Gulch Recharge

Table 4.9: Route 2, Path 4: Empire Gulch: Shallow Aquifer Modeling (mmol/l)

Endmembers	Ca^{+2}	Mg^{+2}	Na^+	SO_4^{2-}	HCO_3^-	Cl^-	SI Calcite	SI Dolomite	SI Gypsum	pH
314638110423401 (Site 13)	1.50	0.25	0.27	0.08	3.11	0.37	0.103	-1.063	-2.708	7.54
Empire Ranch (Site 18)	1.13	0.28	0.64	0.11	3.15	0.29	0.114	-0.346	-2.535	7.71
Change	-0.37	0.03	0.37	0.03	0.04	-0.12	0.011	0.717	0.173	0.17

Table 4.10 presents the adjusted chemical budget required for balancing mass on chloride.

Table 4.10: Route 2, Path 4: Empire Gulch:
Shallow Aquifer Dilution Adjustments (mmol/l)

Endmembers	Ca^{+2}	Mg^{+2}	Na^+	SO_4^{2-}	HCO_3^-	Cl^-
314638110423401 (Site 13)	1.17	0.20	0.21	0.06	2.44	0.29
Empire Ranch (Site 18)	1.13	0.28	0.64	0.11	3.15	0.29
Change	-0.04	0.08	0.43	0.05	0.71	0.00

The significant dilution factor (0.78) is not likely to result from infiltration of dilute waters

due to the large depth to the water table (>220 feet). Instead, mixing with another water

assumed to be dilute in all other constituents is assumed to take place. Given the paucity

of the data, no other alternative is available for modeling this flowpath.

The net increase in bicarbonate (0.71 mmol/l) cannot be accounted for through

calcite dissolution because this mineral is oversaturated at both endmembers. Increases in

pH suggest that calcite precipitation takes place along the gradient as supported by

decreases in calcium. By constraining modeling to calcite precipitation, only one mass

balance model is generated (Table 4.11).

Table 4.11: Route 2, Path 4:
Empire Gulch, Shallow Aquifer Model (mmol/l)

PHASE	1[1]
Calcite	-0.39634
Dolomite	0.29833
Gypsum	0.05123
CO_2	0.49321
X-Ca-Na	
X-Ca-Mg	
X-Mg-Na	0.21425

[1]Bold indicates selected model(s).

Results from Model 1 show that increases in bicarbonate (0.71 mmol/l) are

accounted for through dolomite dissolution (0.298 mmol/l) and dissolution of CO_2 gas

(0.493 mmol/l) that, when combined, offset the loss of carbonate generated from the

precipitation of calcite (-0.396 mmol/l). Cation exchange accounts for any surplus in

magnesium generated from the dissolution of dolomite, but the contribution (0.214

mmol/l) is not as significant as other flowpaths which evolve waters further into the

central basin (i.e. Flowpath 3).

This will be the only flowpath modeled for this route since the analyses for other wells downgradient demonstrate significantly larger losses of chloride (>0.15 mmol/l). This may be a consequence of the deep aquifer nature of the analyses for the central basin which may be developing along another flowpath with little or no vertical mixing of shallow waters higher in chloride. An alternative hypothesis is that central basin groundwaters represent mixing with other flowpath waters dilute in chloride. Mixing models were attempted, but none generated valid results. For this reason, modeling to the deep central basin from the Empire Gulch mountain front was not conducted.

Flowroute 3
Oak Tree Canyon Recharge

The Oak Tree Canyon flowroute is characterized by five-miles of fine grained reddish soils and dense groves of oak trees. As with Flowroute 2, this flowroute evolves waters to the margin of the central basin corridor surrounding Cienega Creek (Figure 4.4). The Empire Mountains located north of the Canyon display Paleozoic and Cretaceous sedimentary limestones cut by light-colored porphyry (Chronic, 1995). Larger masses of porphyry form stocks enriched with copper in the Empire Mining District (Chronic, 1995).

Only deep observation wells (> 1,400 feet depth) were available for modeling this flowpath. Consequently, the results from this modeling are hypothesized to represent changes within the deep aquifer as defined in this study.
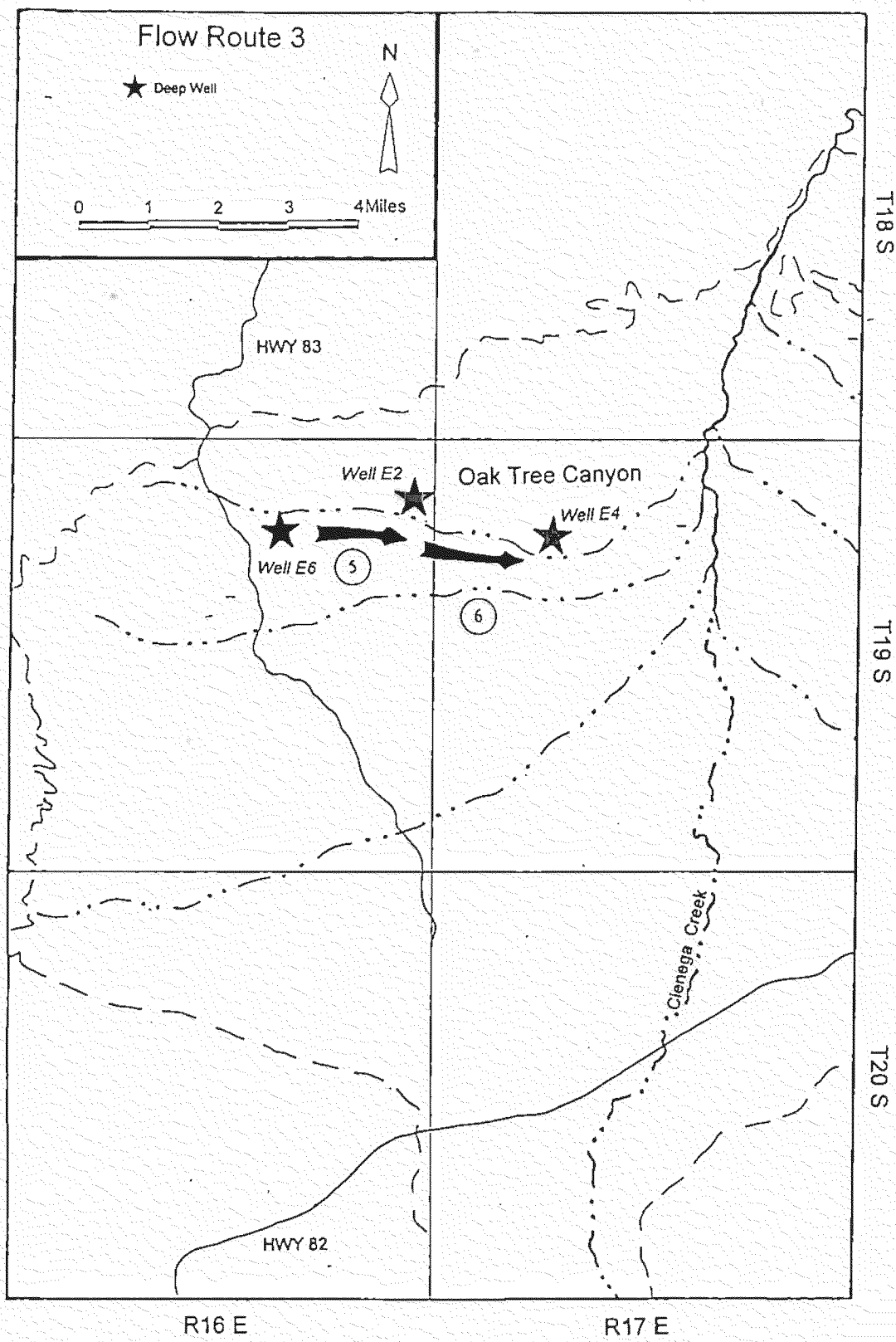
Figure 4.4 Flowroute 3: Oak Tree Canyon Recharge

Flowpath 5
Upper Oak Tree Canyon Alluvium

Endmember Wells E6 (Site 16) and E2 (Site 17) characterize two miles of deep

aquifer flow through Oak Tree Canyon located in the northwest corner of the basin. This

flowpath begins one mile east of Highway 83 and evolves through 2 miles of alluvium.

The relatively small dilution of chloride indicates little mixing along this flowpath. The

chemical budget is presented in Table 4.12.

Table 4.12: Route 3, Path 5: Upper Oak Tree Canyon Chemical Budget (mmol/l)

Endmembers	Ca^{+2}	Mg^{+2}	Na^+	SO_4^{2-}	HCO_3^-	Cl^-	SI Calcite	SI Dolomite	SI Gypsum	pH
Well E6 (Site 16)	0.45	0.20	2.17	0.05	3.38	0.13	-0.341	-1.464	-3.342	7.5
Well E2 (Site 17)	0.65	0.33	1.57	0.05	3.52	0.11	-0.004	-0.755	-3.205	7.7
Change	0.20	0.13	-0.60	0.00	0.14	-0.02	0.337	0.709	0.137	0.2

Due to the slight dilution of chloride, a dilution factor is applied to Well E6 (Table 4.13).

As with other models, it is assumed that mixing water responsible for the dilution are

dilute in all constituents. No other alternative is available given the data. The results are

presented in Table 4.13 on the following page.

Table 4.13: Route 3, Path 5: Upper Oak Tree Canyon Dilution Adjustments (mmol/l)

Endmembers	Ca^{+2}	Mg^{+2}	Na^+	SO_4^{2-}	HCO_3^-	Cl^-
Well E6 (Site 16)	0.38	0.17	1.84	0.04	2.86	0.11
Well E2 (Site 17)	0.65	0.33	1.57	0.05	3.52	0.11
Change	0.27	0.16	-0.27	0.01	0.66	0.00

Although calcite is initially undersaturated, it establishes an almost perfect equilibrium at Well E2 (Table 4.12) which is hypothesized to result from the increase in pH (0.2 units). The decreases in sodium suggest monovalent cation exchange for divalent cations on clays. Although divalent exchange has been observed along other gradients, the relatively large concentration of sodium (2.17 mmol/l) at Well E6 (Site 16) as compared to calcium (0.45 mmol/l) and magnesium (0.20 mmol/l) at Well E2 (Site 17) suggests less competition from divalent cations for sites on clays. Contributions to calcium and sulfate from gypsum dissolution are also negligible due to the small net-concentration change in sulfate (0.01 mmol/l) after accounting for dilution (Table 4.14).

Table 4.14: Route 3, Path 5: Upper Oak Tree Canyon Models (mmol/l)

PHASE	1[1]	2	3	4	5	6	7	8
Calcite	**-0.03651**	0.22966	0.29360	0.29360	0.29360			
Dolomite	**0.16506**	0.03197				0.14680	0.14680	0.14680
Gypsum	**0.00770**	0.00770	0.00770	0.00770	0.00770	0.00770	0.00770	0.00770
CO_2	**0.32148**	0.32148	0.32148	0.32148	0.32148	0.32148	0.32148	0.32148
X-Ca-Na	**-0.13308**		-0.13308		0.03197	-0.13308		-0.11483
X-Ca-Mg			0.16506	0.03197		0.01825	-0.11483	
X-Mg-Na		-0.13308		-0.13308	-0.16506		-0.13308	-0.01825

[1]Bold indicates selected model(s).

Results from Models 1 through 8 differ with respect to the relative contributions of calcite, dolomite, and cation exchange mechanisms. Results from Model 1 differs from Models 2 - 5 results in that the latter suggest a net dissolution of calcite (>0.230 mmol/l) to account for calcite equilibrium, whereas results from Model 1 suggests precipitation (-0.037 mmol/l). Although no models can be excluded, it will be assumed that calcium contributions from cation exchange in conjunction with increases in pH generate equilibrium with calcite. Further contributions from these mechanisms are offset by calcite precipitation in order to maintain the observed equilibrium at the final well. Model 1 in Table 4.14 supports this hypothesis.

Flowpath 6
Lower Oak Tree Canyon Alluvium

This flowpath traverses the next 2 miles of flow along Oak Tree Canyon terminating approximately 3 miles northwest of the start of perennial flow for Cienega Creek. Due to poor accessibility, firsthand characterization of the vegetation and alluvium was not possible, but the USGS quadrangle suggests less vegetation as compared to the previous flowpath. Infiltration or mixing with other flowpaths is also less significant as indicated by conservation of chloride. The chemical budget is presented in Table 4.15 on the following page.

Table 4.15: Route 3, Path 6: Lower Oak Tree Canyon Chemical Budget (mmol/l)

Endmembers	Ca^{+2}	Mg^{+2}	Na^+	SO_4^{2-}	HCO_3^-	Cl^-	SI Calcite	SI Dolomite	SI Gypsum	pH
Well E2 (Site 17)	0.65	0.33	1.57	0.05	3.52	0.11	-0.004	-0.755	-3.205	7.7
Well E4 (Site 20)	1.00	0.34	1.91	0.58	3.49	0.11	-0.128	-1.153	-2.040	7.4
Change	0.35	0.01	0.34	0.53	-0.03	0.00	-0.124	-0.398	1.165	-0.3

The significant increase in sulfate (0.53 mmol/l) suggests that gypsum dissolution is a contributor to the observed increases in calcium (0.35 mmol/l). The imbalance between the calcium and sulfate (0.18 mmol/l) from the dissolution of gypsum is almost perfectly balanced by the required cation exchange with calcium necessary to create the observed change in sodium (0.34 mmol/l). The resulting models are shown in Table 4.16.

Table 4.16: Route 3, Path 6: Lower Oak Tree Canyon Models (mmol/l)

PHASE	1	2	3[1]	4	5	6	7	8
Calcite	-0.00994	-0.35017	0.00010	0.00010	0.00010			
Dolomite	0.00502	0.17514				0.00005	0.00005	0.00005
Gypsum	0.52520	0.52520	**0.52520**	0.52520	0.52520	0.52520	0.52520	0.52520
CO_2	0.12513	0.12513	0.12513	0.12513	0.12513	0.12513	0.12513	0.12513
X-Ca-Na	0.17012		0.17012		0.17514	0.17012		
X-Ca-Mg			0.00502	0.17514		0.00497	0.17508	0.17508
X-Mg-Na		0.17012		0.17012	-0.00502		0.17012	-0.00497

[1]Bold indicates selected model(s).

Of the results from these eight models, Models 3, 4, and 5 support this analysis and differ only in cation exchange processes. The relative concentrations of sodium (1.57 mmol/l) to calcium (0.65 mmol/l) and magnesium (0.33 mmol/l) at Well E2 supports

divalent exchange for monovalent sodium on clays. Only Models 3 and 4 exclude

monovalent cation exchange. Of the remaining two, Model 3 is the most reasonable due

to the unlikely complicated cation exchange process necessary in model 4 to balance a

small change in magnesium (0.01 mmol/l).

CHAPTER 5
SPATIAL COMPARISON OF PHASE CONTRIBUTIONS

Through the use of NETPATH, flowpath modeling presents the contributions of mineral phases to water quality along assumed independent flowpaths. These flowpaths will now be used to evaluate the basin as a system through a quantitative comparison-contrast of phase contributions to geographic location. In describing the geographic evolution of basin groundwaters, the chemistry of Cienega Creek can be qualitatively recreated. This is an important step in corroborating the hypothesis that perennial flows are connected to shallow basin groundwaters and evolve under the same geochemical controls. Corroboration of this hypothesis has obvious implications for management of the Upper Cienega Creek Basin under the multiple use guidelines of the Safford District Management Plan.

Groundwater Evolution

In summarizing the evolution of groundwater along the hydraulic gradient of the RCA, three chemical evolutions have been considered. The first examines the evolution of mountain front recharge to the shallow aquifer surrounding the central-basin corridor of Cienega Creek (Flowpaths 1 and 4); the second suggests the evolution of mountain front recharge through the deep aquifer of the central basin (Flowpath 3); and the third evolves water through the deep aquifer of north-central region of the Cienega Creek corridor (Flowpaths 5 and 6). Due to the relative distribution of deep and shallow wells (Figure 3.5), no models were generated for the evolution of mountain front recharge to the

shallow aquifer of the central basin. A comparison of model results is presented in Table

5.1:

Table 5.1: Phase Contributions (mmol/l)
Mountain Front vs. Central Basin Flowpaths

Location	Gardner Canyon (Flowroute 1)	Empire Gulch (Flowroute 2)	Gardner Canyon (Flowroute 1)	Oak Tree Canyon (Flowroute 3)	
Phase	Mountain Front To Shallow Basin Margin (Flowpath 1)	Mountain Front To Shallow Basin Margin (Flowpath 4)	Mountain Front To the Deep Central Basin (Flowpath 3)	Deep Central Basin Margin Evolution (Flowpath 5)	Deep Central Basin Margin Evolution (Flowpath 6)
Calcite		-0.39634	-0.36413	-0.03651	0.00010
Dolomite	0.03565	0.29833		0.16506	
Gypsum	0.05149	0.05123	0.06593	0.00770	0.52520
CO_2	-0.01978	0.49321	-0.19849	0.32148	0.12513
X-Ca-Na			0.76477	-0.13308	0.17012
X-Ca-Mg	-0.04766		-0.30871		0.00502
X-Mg-Na	0.11386	0.21425	-		

Table 5.1 demonstrates some significant geographic differences with respect to phase

contributions. Specifically, Flowpath 3 suggests a high degree of cation exchange (total

1.074 mmol/l) for the evolution of mountain front recharge through the deep central basin.

This contrasts with Flowpaths 1 and 4 that show smaller total contributions (total 0.376

mmol/l) for waters evolving no further then the shallow central basin margin. This

suggests that clays play a significantly greater role in controlling water quality for the deep

central basin aquifer as compared to shallow aquifer of the surrounding foothills. This is

further corroborated by comparing deep central basin water-types to that of the shallow

wells surrounding the central basin margin (Appendix 5). Specifically, deep central basin

waters are generally of a sodium-bicarbonate type while those of the surrounding foothills

are of a calcium bicarbonate type. Cation-exchange of calcium for sodium is a reasonable

mechanism for evolving calcium dominated waters into sodium dominated waters of the

central basin. In order for cation-exchange to take place, clays must be present in the

central basin to provide surface sites for the exchange. The assumption regarding the

presence of clays is reasonable for this basin following Robertson (1991). In the 28 basins

in the RASA study, Robertson observed:

> "The amount of fine grained silt or clay material (less than 0.0625 mm
> in diameter) near the basin margins ranges from about 10 to 50 percent,
> but may increase toward the center of the basin to more than 90 percent."

Phase contributions from gypsum dissolution and calcite precipitation also demonstrate a

characteristic geographic distribution. Gypsum dissolution (0.525 mmol/l) is significantly

more important for waters evolving through the north-central basin (Flowpath 6) as

compared to those evolving along the hydraulic gradient in the south (all others).

Flowpaths 5 and 6 in the south also demonstrate less calcite precipitation (< 0.037 mmol/l)

or losses to calcium through cation exchange (net loss of 0.004 mmol/l). These

observations suggest larger concentrations of calcium through gypsum dissolution for

waters evolving through the north-central basin as opposed to those of the south. The

relatively larger concentrations of calcium in the north, and the observed increases in

sodium along the hydraulic gradient in the south are important for describing the chemistry

of Cienega Creek as will be discussed.

Sources and Evolution of Cienega Creek Perennial Flow

According to the USGS Spring Water Quadrangle, the perennial flows of Cienega

Creek start at an elevation of approximately 4,440 feet msl (T19S, R17E,s15ddb). The

potentiometric surface in Figure 2.3 suggests that these flows result from an intersection

of the land surface with the water table. This observation alone supports the hypothesis

that Cienega Creek is hydraulically connected to the shallow central basin groundwaters.

However, direct flowpath modeling through the use of Cienega Creek as an endmember

will not produce valid models since perennial flows likely represent mixing of more than

two flowpaths (Figures 2.2 and 2.3). These conclusions derived from flowpath modeling

are used to qualitatively describe the chemical nature of Cienega Creek surface flows. In

doing so, not only is the connection between groundwaters and perennial flows supported,

but the evolution of source waters from the same mountain front recharge is suggested.

This has important management implications since pumping near the mountain front may

adversely affect the (source of) baseflow for Cienega Creek.

Table 5.2 compares shallow groundwater analyses of flowpath endmembers to

analyses for the perennial flows of Cienega Creek. Sample sites may be referenced on

Figure 3.5. Appendix 4 presents the full water quality database for ADEQ Cienega Creek

sampling site (Site 32) compiled over a 2 year period for which averages are presented in

Table 5.3.

Table 5.2: Shallow Flowpath Evolution to Cienega Creek Perennial Flow

Location	Cations mmol/l (% charge)			Anions mmol/l (% charge)			Water Type	
Shallow Aquifer Analyses/ Surface Water Analyses	Ca^{+2}	Mg^{+2}	Na^+	SO_4^{-2}	HCO_3^-	Cl^-	pH	Anions/ Cations
Well 314410110401001 (USGS analyses- Site 4)	1.05 (65)	0.34 (21)	0.43 (14)	0.08 (6)	2.46 (90)	0.11 (4)	7.58[1]	Ca-HCO_3
Empire Ranch Well (Field sample- Site 18)	1.13 (65)	0.28 (16)	0.64 (19)	0.11 (5)	3.64 (90)	0.22 (5)	7.71	Ca-HCO_3
Cienega Creek (Field sample- Site 31)	1.57 (48)	0.50 (15)	2.32 (36)	0.23 (6)	6.41 (91)	0.21 (3)	8.05	Mixed- HCO_3
Cienega Creek ADEQ Site (Field sample- Site 32)	1.24 (51)	0.32 (13)	1.71 (35)	0.37 (14)	4.42 (83)	0.19 (3)	8.19	Ca-HCO_3
Cienega Creek Weir (Field sample- Site 33)	1.25 (51)	0.34 (13)	1.73 (35)	0.36 (14)	4.33 (82)	0.21 (4)	8.52	Ca-HCO_3

[1]Parameter estimated via equilibrium with calcite

Table 5.3: Cienega Creek Analyses, Site 32 (T18S-R17E- sec14 dad).
ADEQ Average Data for Two Year Period (11/91 - 8/93)

Location	Cations (mmol/l) Average (Std. Dev.)			Anions (mmol/l) Average (Std. Dev.)			Water Type	
ADEQ Data Perennial Flows	Ca^{+2}	Mg^{+2}	Na^+	SO_4^{-2}	HCO_3	Cl-	pH	Anions/ Cations
Cienega Creek ADEQ Site (Site 32)	1.44 (0.08)	0.37 (0.04)	2.04 (0.14)	0.42 (0.03)	4.23 (0.34)	0.22 (0.06)	8.03 0.21	Ca-HCO_3

The strongest correlation between surface water chemistry and groundwater evolution is the relatively high sodium concentrations (>2.04 mmol/l) measured in the perennial flows of Cienega Creek. The high sodium in Cienega Creek contrasts significantly with the sodium analyses for shallow groundwater endmembers located along the central basin margin (<0.65 mmol/l). This suggests that the calcium-sodium and magnesium-sodium cation exchange used to explain the evolution of shallow aquifer

waters to the deep aquifer in the central basin (Flowpath 3) also contributes to the water quality of Cienega Creek.

This mechanism accounts for increases in sodium, but does not explain the conservation of calcium for perennial flows (>1.24 mmol/l) with respect to the shallow wells located outside the central basin margin (>1.05 meq/l). Although magnesium-sodium cation exchange is likely contributing to the high sodium signature, calcium-sodium cation-exchange should also be taking place. Therefore, a secondary source of calcium is required for conservation of this cation in the perennial flows of Cienega Creek. Flowpath 6 (Oak Tree Canyon) is a reasonable source of calcium since this flowpath demonstrates a significant amount of gypsum dissolution (0.525 mmol/l) without subsequent calcium-sodium cation exchange or calcite precipitation (Table 5.3). Use of this deep-aquifer flowroute to explain the contribution of calcium requires the assumption that gypsum dissolution is also taking place in the shallow aquifer of the northern basin. This is supported by a larger concentration of sulfate in perennial flows (>0.23 mmol/l) as compared to shallow flowpath endmembers of the southern basin (<0.11 mmol/l). In this study, it is assumed that the only source of sulfate is from gypsum dissolution.

Although gypsum is a likely contributor to perennial flow chemistry, the relatively large molar imbalance between calcium and sulfate in surface waters (>1.34 mmol/l) in favor of calcium requires additional source for this cation. WATEQ4F output indicates that perennial flows are supersaturated in carbonate minerals. Therefore, contributions to calcium from the dissolution of calcite (i.e. through buffering of acidity generated from CO_2 gas dissolution) is not likely. Since gypsum dissolution alone (Flowroute 3) cannot

account for the imbalance between calcium and sulfate, contributions from another

flowpath endmember must be identified. Shallow Well 30 (Table 5.4) located within the

shallow Cienega Creek corridor in the eastern basin represents a candidate for the

hypothesized calcium influx.. Table 5.4 presents the analyses for this well from a field

sample.

Table 5.4: Shallow Aquifer Analyses for Cienega Ranch Well, Eastern-Central Basin

Location	Cations mmol/l (% charge)			Anions mmol/l (% charge)			Water Type	
Eastern Basin Cienega Creek Corridor Shallow Well Analyses	Ca^{+2}	Mg^{+2}	Na^+	SO_4^{-2}	HCO_3	Cl-	pH	Cation/ Anion
Cienega Ranch Well (Field Sample - Site 30)	1.59 (57)	0.43 (15)	1.55 (28)	0.18 (7)	4.68 (88)	0.24 (5)	7.54	Ca-HCO$_3$

[1]Parameter estimated via equilibrium with calcite

Due to lack of data for the eastern basin, a flowpath evolving waters to this endmember

(Cienega Ranch Well) was not generated. The saturation indices as calculated by

WATEQ4F for the field sample analyses indicates that calcite is supersaturated (SI =

0.222). For this reason, contributions to calcium and carbon via calcite dissolution are not

feasible. Dolomite, however, is undersaturated (SI = -0.689) and may be the source of the

relatively high calcium (1.59 mmol/l) and bicarbonate (4.68 mmol/l) concentrations for

analyses of a field sample of this shallow well. Dolomite dissolution may also explain the

relatively high sodium concentration (1.55 mmol/l) resulting from magnesium-sodium

cation exchange, and supported by the low concentration of magnesium (0.43 mmol/l)

relative to calcium (1.59 mmol/l). These observations suggest that the eastern basin also contributes both to the chemistry and baseflow of Cienega Creek.

Lastly, the high chloride concentration (0.24 mmol/l) in Cienega Creek perennial flows is consistent with chloride content of most shallow well analyses (Appendix 5). This further supports the hypothesis that the shallow aquifer is hydraulically connected to Cienega Creek, and that baseflow has its origin mountain front recharge. It must be emphasized that this conclusion does not exclude a hydrologic connection between Cienega Creek and the deeper aquifer. The lack of a regional confining clay strata suggests that the shallow aquifer is connected to the deeper aquifer. Thus, pumping from the latter could affect Cienega Creek baseflow directly. Mechanisms responsible for the difference in chloride were suggested in previous sections.

CHAPTER 6
RECOMMENDATIONS AND CONCLUSIONS

Recommendations for Further Study

In this study, mass balance models were generated which suggest that the geochemistry of the Upper Cienega Creek Basin is typical of alluvial aquifers in the southwest. However, due to lack of pH data and isotopic analyses, flowpaths are poorly constrained and thus generated a set of non-unique solutions. Aside from elimination by testing against thermodynamic criteria, the only other way to reduce the number of feasible solutions is introducing new data on the chemistry of the system. This data might include mineralogical and petrographic information identifying which of the plausible phases are present along each flowpath, and visual evidence as to which minerals are reactants or products in the system (Plummer, et al., 1982). The following are some suggestions for improving both the quality and confidence of geochemical models generated for this basin.

With respect to the Upper Cienega Creek Basin, it was assumed that dolomite consists of a 1:1 ratio of carbon to magnesium. Naturally occurring dolomite, however, deviates somewhat from this ratio ranging from 58:42 to 47½:52½ for calcium to magnesium (Klein and Hurlbut, 1985). X-ray defraction analysis for dolomite samples and a corrected stoichiometric definition for this phase in the NETPATH database will generate more accurate mass transfer models. For example, most models demonstrate dolomite dissolution to account for increases in magnesium along the flowpath. Smaller contributions of magnesium from calcium-enriched dolomite (58:42) may require

increased dissolution of this phase to balance increases in magnesium. Accordingly, greater contributions of calcium may minimize or even eliminate models demonstrating small contributions of calcite dissolution for increases in calcium along the gradient. This would corroborate Robertson's observations regarding calcite precipitation (vs. calcite dissolution) for small increases in pH (i.e. Flowpaths 5, 6).

Isotopic analyses for carbon and sulfur at endmember wells serves as an additional constraint for eliminating models. To use isotope mass balance constraints for modeling, the isotopic compositions of appropriate source phases (i.e. calcite, dolomite, gypsum, and pyrite) would be determined. These compositions are then defined in the NETPATH database as phase constraints. Analyses for the isotopic composition of endmember waters ($\delta^{34}S$, $\delta^{13}C$) must also be determined and specified as analytical constraints. For dissolution of a particular isotope, NETPATH will calculate mass balance models in the same way discussed in Chapter 3 (i.e. congruent dissolution of a mineral phase). For precipitation of a particular isotope, NETPATH uses published fractionation factors for modeling of both the Carbon-13 and Sulfur-34 systems. With this information, suggested mass balance models in this study can be checked by verifying that phase dissolution will generate the observed change in the isotopic composition of endmember waters. If a reasonable model fails to generate mass balance for the isotopic composition of endmember wells, uncertainties in the isotopic compositional data of selected phases may be refined for convergence on a reasonable unique solution. Isotopic analyses were not considered for this study due to the high cost associated with mass spectrometry analyses. Isotopic analysis can also help identify the carbon in Cienega Creek since modern carbon

(from the degradation of organic debris) should have a distinguishable C-14 signature whereas fluxes from carbonate mineralogy dissolution will be composed of (dead) C-12.

Of obvious significance is the lack of pH data for many of the shallow endmember wells in the USGS database. In addition, no protocol is included with analyses for the Harshbarger report (1975); it is unclear whether the reported pH and alkalinity measurements were conducted in the field or lab. Both CO_2 out-gassing and changes in temperature could be significant in affecting reported concentrations of calcium and saturation indices for calcite. For this reason, field measurements of pH and alkalinity data would be useful for corroborating published data.

A comparison of chemical analyses for deep and shallow wells demonstrate consistent differences with respect to sodium and chloride. Nevertheless, conclusions with respect to the hydrologic independence of the deep and shallow aquifer should not be made without further study. The non-uniform geographic distribution of deep and shallow wells suggests that water quality differences may be areal in nature. It would be useful to check this hypothesis by sampling shallow wells within the four mile wide corridor surrounding Cienega Creek and comparing these analyses against those of the deep wells listed in Appendix 5. If differences in water quality prove to be independent of areal distribution, nested piezometers may be used to identify any vertical gradients. If these exist, chemical modeling through NETPATH may explain the evolution responsible for changes in water quality with depth. Corroboration of a hydrologic link between the shallow and deep aquifer may be extended to Cienega Creek since potentiometric data and NETPATH modeling supports a link between the shallow aquifer and perennial flows.

In this study, not all wells of interest were sampled as a result of difficulties regarding access. For future studies, it is recommended that a general form letter be mailed out to registered well owners offering a free chemical analyses in exchange for permission to sample a respective well on a given date. Well locations, well depths, and addresses of registered well owners may be obtained from the well registration report available from the ADWR in Tucson.

Due to the paucity of data, disputable assumptions regarding flowpath chemistry were made so that modeling could be completed. For example, loss of chloride along a given flowpath required a mixing source dilute in all other constituents. Although mixing is likely taking place, it may contain other constituent ions aside from chloride. These were not considered in the modeling.

The qualitative nature of the modeling is best demonstrated by Flowpath 4 which shows exclusive magnesium-sodium ion exchange on clays. Although it is hypothesized that cation-exchange is responsible for the increases in sodium, it is not likely to be exclusive to magnesium since calcium is also in the system. NETPATH may not realize calcium-sodium exchange since losses in calcium are modeled through calcite precipitation unconstrained by a system open to CO_2 influx. In fact, losses in calcium probably result from a combination of both calcite precipitation and calcium-sodium ion exchange. For this reason, modeling should be considered qualitative at best.

Conclusions

This study has evaluated mountain-front recharge from the Santa Rita Mountains through the western alluvium of the Upper Cienega Creek Basin. The first objective was

to qualitatively identify the natural geochemical processes affecting basin groundwater quality. The second objective was to geographically compare these processes in space in order to identify any obvious trends that could be used to explain the surface water chemistry of Cienega Creek. In doing so, conclusions about the source and evolution of Cienega Creek waters are derived.

Mass balance modeling shows that the basic chemical processes identified by Robertson (1991) may be used to describe the geochemical evolution of basin waters in the Upper Cienega Creek Basin. These include increases in pH accounted for by the weathering of silicates (ranging between 7.4 and 8.4), subsequent precipitation of calcite, dissolution of dolomite, dissolution of gypsum, and cation exchange of calcium for sodium. Although mass balance calculations indicate that these processes are possible, mass balance solutions are non-unique.

Spatially, waters evolve from a calcium-bicarbonate type at the mountain front to a sodium-bicarbonate type in the central basin. Analyses for Cienega Creek perennial flows demonstrate a relatively high sodium concentration (greater than 1.71 meq/l) characteristic of central basin groundwaters. Given the similar chemical composition, it is assumed that both surface and groundwaters evolve under the same geochemical controls while originating from the same mountain-front recharge sources. Although groundwater data for the eastern basin was sparse, the mineralogy of the Whetstone Mountains is similar in composition to that of the Santa Ritas. As such, the models presented here are also hypothesized to qualitatively represent the evolution of eastern basin groundwaters.

Appendix 2

Chemical Data for Upper Basin

Major Cations/Anions

SID	Name	Na mg/l	Na meq/l	K mg/l	K meq/l	Mg mg/l	Mg meq/l	Ca mg/l	Ca meq/l	Cl mg/l	Cl meq/l	SO4 mg/l	SO4 meq/l	HCO3 mg/l	HCO3 meq/l	CO3 mg/l	CO3 meq/l	NO3 mg/l	NO3 meq/l	% IMB
1	Apache Springs 1	10.0	0.43	grp		24.0	1.98	78.00	3.89	7.00	0.20	4.90	0.10	310.0	5.08	0.00	0.00			7.8
2	314230110424801	2.51	0.11	grp		7.00	0.58	42.00	2.10	4.00	0.11	7.40	0.15	130.0	2.13	12.0	0.40			-0.29
3	314439110415701	10.0	0.43	grp		9.20	0.76	56.00	2.79	4.00	0.11	16.0	0.33	190.0	3.11	0.00	0.00			5.66
4	314341110402801	1.80	0.08	grp		6.60	0.54	42.00	2.10	1.00	0.03	5.30	0.11	160.0	2.62	0.00	0.00			-0.82
5	314410110402101	10.0	0.43	grp		8.30	0.68	42.00	2.10	4.00	0.11	7.40	0.15	150.0	2.48	0.00	0.00	0.10	0.00	8.23
6	314410110401001	2.10	0.09	grp		7.00	0.58	36.00	1.80	1.00	0.03	12.0	0.25	130.0	2.13	0.00	0.00			1.14
7	314412110385501	10.0	0.43	grp		9.20	0.76	55.00	2.74	10.0	0.28	13.0	0.27	180.0	2.95	0.00	0.00			5.83
8	Obs. Well E14	27.0	1.17	3.70	0.09	10.0	0.82	27.00	1.35	4.00	0.11	5.00	0.10	201.0	3.29	0.00	0.00	1.30	0.02	-2.09
9	Obs. Well E5	40.0	1.74	3.00	0.08	6.20	0.51	27.00	1.35	4.00	0.11	13.0	0.27	198.0	3.24	0.00	0.00	0.60	0.01	-0.25
10	314540110444401	7.90	0.34	grp		24.2	1.98	54.00	2.69	10.0	0.28	67.0	1.39	190.0	3.11	0.00	0.00			2.27
11	Greaterville Spring	50.2	2.18	0.86	0.02	27.1	2.23	93.70	4.68	25.2	0.71	30.7	0.64	526.0	8.62	3.20	0.11	0.50	0.01	-5.07
12	Greaterville Well	27.2	1.18	1.60	0.04	16.1	1.33	54.20	2.70	16.7	0.47	81.6	1.70	197.0	3.23	3.20	0.11	0.50	0.01	-2.43
13	314638110423401	6.20	0.27	grp		6.10	0.50	60.00	2.99	13.0	0.37	7.40	0.15	190.0	3.11	0.00	0.00			1.77
14	Los Posos Tank	15.0	0.65	<1		6.80	0.56	52.10	2.60	20.0	0.56	3.90	0.08	156.0	2.56	0.00	0.00	5.56	0.09	7.32
15	Rex Allen	13.4	0.58	<1		6.23	0.51	47.50	2.37	10.1	0.28	8.76	0.18	182.0	2.98	0.00	0.00	7.16	0.12	-8.45
16	Obs. Well E6	50.0	2.17	3.00	0.08	4.70	0.39	18.00	0.90	4.60	0.13	5.00	0.10	206.0	3.38	0.00	0.00	0.40	0.01	-1.71
17	Obs. Well E2	36.0	1.57	2.80	0.07	8.00	0.66	26.00	1.30	4.00	0.11	5.00	0.10	215.0	3.52	0.00	0.00	1.90	0.03	-3.05
18	Empire Ranch	14.7	0.64	<1		6.80	0.56	45.00	2.25	7.81	0.22	10.5	0.22	192.0	3.15	0.00	0.00	5.35	0.09	-2.31
19	Empire Gulch	21.6	0.94	1.89	0.05	10.7	0.88	58.60	2.92	8.35	0.24	14.4	0.30	273.0	4.47	0.00	0.00	1.00	0.02	-2.66
19	Empire Gulch 2	26.9	1.17	<1		11.9	0.98	68.70	3.43	11.4	0.32	36.6	0.76	305.0	3.15			2.27	0.04	-5.38
20	Obs. Well E4	44.0	1.91	3.10	0.08	8.10	0.67	40.00	2.00	4.00	0.11	55.0	1.15	213.0	3.49	0.00	0.00	1.90	0.03	-1.87
21	Obs Well E7	70.0	3.04	1.70	0.04	2.20	0.18	12.00	0.60	5.30	0.15	56.0	1.17	150.0	2.46	0.00	0.00	6.20	0.10	-1.66
22	Obs. Well E3	67.0	2.91	21.0	0.54	0.70	0.06	15.00	0.75	4.00	0.11	75.0	1.56	133.0	2.18	0.00	0.00	1.90	0.03	3.61

Major Cations/Anions

SID	Name	Na mg/l	meq/l	K mg/l	meq/l	Mg mg/l	meq/l	Ca mg/l	meq/l	Cl mg/l	meq/l	SO4 mg/l	meq/l	HCO3 mg/l	meq/l	CO3 mg/l	meq/l	NO3 mg/l	meq/l	% IMB
23	Obs. Well E1	220.0	9.57	4.40	0.11	0.20	0.02	85.00	4.24	12.0	0.34	627.0	13.1	10.0	0.16	7.80	0.26	8.30	0.13	-0.9
24	Empire Gulch Well	59.50	2.59	<1		0.50	0.04	7.89	0.39	3.82	0.11	36.20	0.75	141.0	2.32	0.00	0.00	0.30	0.00	4.41
25	Obs. Well E9	70.00	3.04	3.70	0.09	0.80	0.07	8.00	0.40	4.00	0.11	28.00	0.58	136.0	2.23	20.4	0.68	1.60	0.03	-2.79
26	Obs. Well E8	41.00	1.78	1.60	0.04	6.20	0.51	17.00	0.85	4.60	0.13	5.00	0.10	182.0	2.98	0.00	0.00	1.20	0.02	-1.49
27	Obs. Well E10	56.00	2.44	1.40	0.04	2.00	0.16	11.00	0.55	4.00	0.11	24.00	0.50	160.0	2.62	0.00	0.00	0.40	0.01	-1.62
28	Obs. Well E11	45.00	1.96	3.60	0.09	4.60	0.38	19.00	0.95	4.00	0.11	5.00	0.10	196.0	3.21	0.00	0.00	3.30	0.05	-2.17
29	Obs. Well E12	38.00	1.65	3.90	0.10	10.9	0.90	35.00	1.75	10.0	0.28	9.00	0.19	235.0	3.85	0.00	0.00	3.50	0.06	-0.45
30	314938110353601	34.00	1.48	grp		9.00	0.74	50.00	2.50	7.00	0.20	16.00	0.33	250.0	4.10	0.00	0.00			0.7
30	Cienega Ranch	35.70	1.55	<1		10.3	0.85	63.60	3.17	8.53	0.24	17.00	0.35	285.0	4.68	0.00	0.00	2.20	0.04	2.47
31	Cienega Crk	53.30	2.32	1.19	0.03	12.0	0.99	62.70	3.13	7.30	0.21	22.30	0.46	391.0	6.41	0.00	0.00	0.50	0.01	-4.75
32	Cienega Crk Fnc	39.30	1.71	2.32	0.06	7.83	0.64	49.70	2.48	6.80	0.19	35.00	0.73	270.0	4.42	0.00	0.00	0.72	0.01	-4.79
33	Cienega Crk Weir	39.80	1.73	1.89	0.05	8.25	0.68	50.00	2.50	7.28	0.21	34.60	0.72	264.0	4.33	0.00	0.00			-3.2
34	Sawmill Canyon	12.60	0.55	1.57	0.04	6.79	0.56	46.40	2.32	7.39	0.21	10.30	0.21	171.0	2.80	3.20	0.11	0.50	0.01	1.77
35	Wrightson Snow	0.00	0.00	0.00	0.00	0.00	0.00	0.00	0.00	1.23	0.03	0.00	0.00	36.0	0.59	3.20	0.11			ADJ
36	Cienega Creek 1	33.95	1.48	1.83	0.05	8.08	0.67	57.20	2.85	3.99	0.11	17.30	0.36	269.0	4.41	0.00	0.00	1.90	0.03	1.32
37	Cienega Crk 2	37.70	1.64	1.64	0.04	7.89	0.65	51.90	2.59	4.45	0.13	20.20	0.42	254.0	4.16	0.00	0.00	1.52	0.02	1.95
38	Cienega Crk 3	37.70	1.64	2.19	0.06	7.96	0.66	48.90	2.44	4.65	0.13	22.20	0.46	245.0	4.02	0.00	0.00	1.31	0.02	1.71
39	Cienega Crk 4	43.30	0.00	1.73	0.04	8.39	0.69	54.50	2.72	5.37	0.15	27.80	0.58	269.0	4.41	0.00	0.00	0.78	0.01	1.66
40	Cienega Crk 5	43.90	1.91	2.49	0.06	8.34	0.69	51.60	2.57	5.42	0.15	28.80	0.60	266.0	4.36	0.00	0.00	0.55	0.01	1.09
41	Hidden Valley	30.20	1.31	3.08	0.08	12.7	1.05	64.80	3.23	8.17	0.23	30.20	0.63	323.0	5.29	3.20	0.11	0.50	0.01	-5.05
42	Apache Springs 2	6.69	0.29	1.18	0.03	18.8	1.55	78.70	3.93	8.35	0.24	14.40	0.30	336.0	5.51	0.00	0.00	1.88	0.00	-4.27
43	313910110422501	2.60	0.11	0.18	0.00	65.0	5.35	290.0	14.5	5.00	0.14	760.0	15.8	230.0	3.77	0.00	0.00			0.5
44	BLM Well	76.00	3.31	0.50	0.01	0.20	0.02	3.40	0.17	4.00	0.11	13.00	0.27	192.0	3.15	0.00	0.00	0.40	0.01	-0.5

Additional Information

SID	Name	Date	Source	Type	Location	USGS Quad	Elev	Hd	Dpth	Alk fld	Alk lab	pH fld	pH lab	EC	T
1	Apache Springs 1	4/17/41	USGS WRC	Spring	20-16-6dcb	Sonoita	5190	5188	10	250		7.40		491	22
2	314230110424801	4/18/41	USGS WRC	Well	20-16-9dbb	Sonoita	5200	4800	540	126		(7.59)		244	(25.0)
3	314439110415701	4/15/41	USGS WRC	Well	19-16-34ba	Sonoita	4900	4775	230	154		(7.45)		318	
4	314341110402801	9/24/41	USGS WRC	Well	20-16-2aaa	Sonoita	4800	4684	116	129		(7.58)		257	18.8
5	314410110402101	4/15/41	USGS WRC	Well	19-16-35dad	Sonoita	4740	4710	101	124		(7.60)		254	19
6	314410110401001	9/20/41	USGS WRC	Well	19-16-36cb	Sonoita	4725	4701	175	107		(7.83)		230	18.5
7	314412110385501	4/15/41	USGS WRC	Well	19-17-31ca	Sonoita	4635	4596	42	144		(7.53)		312	18
8	Obs. Well E14	2/15/75	Harshbarger	Well	20-17-15dcd	Elgin	4764	4620	2000		167		7.60	330	25.6
9	Obs. Well E5	10/19/74	Harshbarger	Well	19-17-21ddd	Spring	4533	4479	1480		165		7.70	310	22.9
10	314540110444401	9/24/41	USGS WRC	Well	19-16-19dc	Empire	5200	5178	24	157		(7.53)		522	20.5
11	Greaterville Spring	3/31/95	Field	Spring	19-16-19daa	Empire	5250				439	7.84		850	10.1
12	Greaterville Well	3/31/95	Field	Well	19-16-16cbb	Empire	5120	4670	472		162	8.27		492	13.8
13	314638110423401	9/24/41	USGS WRC	Well	19-16-16ddb	Empire	4931	4703	365	157		7.54		37	20.5
14	Los Posos Tank	3/4/96	Field	Well	19-16-22abd	Empire	4990	4725	365	128	172	7.60			17
15	Rex Allen	3/4/96	Field	Well	19-16-16ddc	Empire	4960	4675	365	149	182	7.54			19
16	Obs. Well E6	10/11/74	Harshbarger	Well	19-16-11bbb	Spring	4939	4695	1510		172		7.50	340	26.1
17	Obs. Well E2	9/21/74	Harshbarger	Well	19-16-12aac	Empire	4722	4636	1500		179		7.70	340	22.8
18	Empire Ranch	3/4/96	Field	Well	19-17-18aca	Empire	4620		220	157	182	7.71			17.5
19	Empire Gulch	10/15/96	Field	Spring	19-17-10bdc	Spring	3385			217	216	7.77		452	21.7
19	Empire Gulch 2	3/7/96	Field	Spring	19-17-10bdc	Empire	4580			250		6.85			18
20	Obs. Well E4	9/27/74	Harshbarger	Well	19-17-8cb	Empire	4563	4434	1460		177	7.40		450	21.7
21	Obs Well E7	10/25/74	Harshbarger	Well	19-17-9abb	Spring	4521	4470	1285		125	7.30		380	21.2
22	Obs. Well E3	11/7/74	Harshbarger	Well	19-17-20acb	Empire	4559	4558	1865		111	7.80		360	31.7

Additional Information

SID	Name	Date	Source	Type	Location	USGS Quad	Elev	Hd	Dpth	Alk		pH		EC	T
										fld	lab	fld	lab		
23	Obs. Well E1	10/2/74	Harshbarger	Well	19-17-17bbb	Empire	4750	4593	1500			8.5		1360	29
24	Empire Gulch Well	3/4/96	Field	Well	19-17-17bbb	Empire	4539	845		116	157	8.24			18
25	Obs. Well E9	11/27/74	Harshbarger	Well	19-17-10bad	Spring	4386	4323	1412		113	8.4		320	26.1
26	Obs. Well E8	11/8/74	Harshbarger	Well	19-17-15bbd	Spring	4495	4418	1220		152	7.3		290	22.3
27	Obs. Well E10	12/6/74	Harshbarger	Well	19-17-23aad	Spring	4451	4419	1500		133	6.4		320	26.2
28	Obs. Well E11	12/22/74	Harshbarger	Well	19-17-14ada	Spring	4465	4398	1608		163	7.4		320	27.3
29	Obs. Well E12	1/22/75	Harshbarger	Well	19-17-1ccd	Spring	4393	4329	1293		196	7.9		400	25
30	314938110353601	3/23/51	USGS WRC	Well	18-17-35bc	Spring	4320		200	207		(7.45)			18.5
30	Cienega Ranch	3/4/96	Field	Well	18-17-35abc	Empire	4370			234	295	7.54			17
31	Cienega Crk Eph	3/26/95	Field	Cienega	19-17-3aac	Spring	4350				321	8.05			16
32	Cienega Crk Fnc	10/15/95	Field	Cienega	18-17-13ccb	Spring	4175			220	221	8.19		395	17.8
33	Cienega Crk Weir	10/15/95	Field	Cienega	18-18-6cdc	Narrows	4125			203	216	8.52		455	17.8
34	Sawmill Canyon	4/3/95	Field	Spring	19-15-33dcd	Wrightson	6350				140	7.54		317	10
35	Wrightson Snow	3/31/95	Field	Snow	20-15-7	Wrightson	9000				30				
36	Cienega Creek 1	2/12/95	Field	Cienega	18-17-13cba	Spring	4175			424	432	8.03	8.26	424	16
37	Cienega Crk 2	2/12/95	Field	Cienega	18-17-13cba	Spring	4165				208	8.22	8.57	401	15.5
38	Cienega Crk 3	2/12/95	Field	Cienega	18-17-12dcc	Spring	4150				201	8.20	8.55	384	17
39	Cienega Crk 4	2/12/95	Field	Cienega	18-17-12dbc	Narrows	4125				221	8.40	8.56	444	20.6
40	Cienega Crk 5	2/12/95	Field	Cienega	18-18-6cdc	Narrows	4100				218	8.48	8.55	437	20.6
41	Hidden Valley	3/26/95	Field	Spring	18-16-16bdb	Empire	4750				265	8.12			14.5
42	Apache Springs 2	10/15/95	Field	Spring	20-16-6dcb	Sonoita	5190			250		7.22			21.7
43	313910110422501	4/16/41	USGS WRC	Well	20-16-33add	Sonoita	4575			189		(6.98)			27
44	BLM Well	10/17/88	ADEQ	Well	19-17-3adb	Spring	4350	4350	749	160					

Appendix 3
Cienega Creek Surface Water Data

Arizona Department of Environmental Quality

Stream Chemical Data
Site ID SC14 - Upper Cienega Creek
Location : T18S-R17E- sec14 dad
Latitude : 31° 51' 53"
Longitude: 110° 34' 1"

Major Cations / Anions

Data	11/26/91 mg/l	1/31/92 mg/l	5/14/92 mg/l	8/6/92 mg/l	11/14/92 mg/l	3/16/93 mg/l	2/27/93 mg/l	8/18/93 mg/l
Ca+2	60.30	63.20	57.60	58.40	52.60	57.90	55.60	55.10
Mg+2	9.40	10.30	9.20	8.35	7.60	10.10	8.50	8.40
Na+	45.10	50.00	45.40	44.00	43.20	53.00	47.90	46.40
K+	1.20	2.40	2.18	2.29	1.77	3.88	2.57	2.40
CO3-2	0.50	7.00	1.00	2.00	4.00	2.00	2.00	2.40
HCO3-	226.00	227.00	265.00	260.00	268.00	284.00	268.00	265.00
Cl-	9.10	9.00	2.60	8.37	8.69	10.00	7.20	8.20
SO4-2	42.00	43.00	35.70	40.60	40.00	38.30	41.30	40.70
NO2+NO3	0.12	0.09	0.10	0.20	0.20	0.12	0.10	0.19
F-	0.36	0.34	0.41	0.39	0.49	0.38	0.45	0.44

Data	11/26/91 meq/l	1/31/92 meq/l	5/14/92 meq/l	8/6/92 meq/l	11/14/92 meq/l	3/16/93 meq/l	2/27/93 meq/l	8/18/93 meq/l
Ca+2	3.01	3.15	2.87	2.91	2.62	2.89	2.77	2.75
Mg+2	0.77	0.85	0.76	0.69	0.63	0.83	0.70	0.69
Na+	1.96	2.17	1.97	1.91	1.88	2.31	2.08	2.02
K+	0.03	0.06	0.06	0.06	0.05	0.10	0.07	0.06
CO3-2	0.02	0.23	0.03	0.07	0.13	0.07	0.07	0.08
HCO3-	3.70	3.72	4.34	4.26	4.39	4.65	4.39	4.34
Cl-	0.26	0.25	0.07	0.24	0.25	0.28	0.20	0.23
SO4-2	0.87	0.90	0.74	0.85	0.83	0.80	0.86	0.85
NO2+NO3	0.00	0.00	0.00	0.00	0.00	0.00	0.00	0.00
F-	0.00	0.00	0.00	0.00	0.00	0.00	0.00	0.00
% IMB	8.48	9.82	4.10	1.28	-4.23	2.53	0.68	-0.07

Field Parameters

Data	11/26/91	1/31/92	5/14/92	8/6/92	11/14/92	3/16/93	2/27/93	8/18/93
pH	7.91	8.34	7.87	7.73	8.00	8.26	8.20	7.95
TDS (mg/l)	300	330	322	294	312	352	318	323
T(C)	14.00	12.50	19.50	18.50	11.00	17.00	18.50	20.50
Fld EC(us)	508	508	503	459	496	564	511	480
Alk (mg/l)	226	234	217	213	213	233	220	221
DO (mg/l)	9.30	11.30	7.80	6.23		8.70	8.53	7.40

Stream Chemical Data

Site ID SC14 - Upper Cienega Creek
Location   T18S-R17E- sec14 dad
Latitude: 31° 51' 53"
Longitude: 110° 34' 1"

Lab	Average (mg/l)	Std Dev (mg/l)
Ca+2	57.59	3.27
Mg+2	8.98	0.93
Na+	46.88	3.29
K+	2.34	0.76
CO3-2	2.61	2.05
HCO3-	257.88	20.57
Cl-	7.90	2.29
SO4-2	40.20	2.29
NO2+NO3	0.14	0.05
F-	0.41	0.05

Field	Average	Std. Dev.
Fld pH	8.03	0.21
TDS (mg/l)	319	18.01
T(C)	16.44	3.50
Fld EC (us)	504	30.11
Alk (mg/l)	222	8.22
DO (mg/l)	8.47	1.60